Highlights

- Shear work affects structure, fat particle size and creep behaviour of cheese.
- Excessive shear work causes loss of anisotropic nature of model Mozzarella cheese.
- Elastic response of model cheese increased with increase in shear work levels.

Changes in creep behavior and microstructure of model Mozzarella cheese during working

<u>Prateek Sharma</u>[1,3*] , Peter A. Munro[1], Graeme Gillies[2], Peter G. Wiles[2], Tzvetelin T. Dessev[1]

[1]*Riddet Institute, Massey University, Private Bag 11222, Palmerston North, New Zealand*

[2]*Fonterra Research and Development Centre, Palmerston North, New Zealand*

[3]*Dairy Technology Division, National Dairy Research Institute, Karnal-132001, Haryana, India*

[*] *Corresponding Author: Tel: +64 635 05545 extn 87010*
Email address: P.Sharma@massey.ac.nz

Abstract

The effect of shear work input on the microstructure, fat particle size and creep behavior of model Mozzarella type cheeses was studied. Cheese samples were prepared in a twin screw cooker at 70 ^{o}C by mixing protein and fat phases together with different amounts of shear work input. Major changes in cheese structure were observed while working at 150 rpm and 250 rpm screw speeds. Confocal microstructures plus macroscopic observations showed systematic changes in structure with increased shear work inputs with unmixed buttery liquid observed at <5 kJ.kg^{-1}, typical Mozzarella type microstructures (elongated fat-serum channels) at 6-15 kJ.kg^{-1} and homogeneously distributed, small size fat droplets at >58 kJ.kg^{-1}. At very high shear work inputs, > 75 kJ.kg^{-1}, striations or anisotropy in the microstructures had disappeared and small micro-cracks were evident. A 4-element Burger's model was found adequate for fitting the creep data of model cheese at 70 ^{o}C but a 6-element model was required at 20 ^{o}C. As shear work input increased retarded compliance decreased and zero shear viscosity increased indicating the more elastic behavior of the cheeses with higher shear work input. Changes in the protein matrix appear to be the main reason for increased elastic behavior.

Key words: Shear work, Microstructure, Retarded compliance, Fat particle size

1. Introduction

The process of Mozzarella cheese manufacture includes a hot-water (60-85 ^{o}C) stretching and working step that is normally carried out with single or twin screw cheese cookers. In this process step proteins in the cheese curd form into large protein strands resembling fibers and fat-serum pools are distributed within this fibrous network (McMahon, Fife, & Oberg, 1999). The presence of the fat-serum channels helps to deliver the desired melt functionality for pizza applications. Numerous studies have been conducted in the recent past using twin screw cookers for the manufacture of imitation cheese (Noronha, O'Riordan, & O'Sullivan, 2008; El-Bakry, Duggan, O'Riordan, & O'Sullivan, 2010a, b), process cheese (Glenn, Daubert, Farkas & Stefanski, 2003; Kapoor, Lehtola, & Metzger, 2004) and Mozzarella cheese (Mulvaney, Rong, Barbano, & Yun, 1997; McMahon et al., 1999; Yu & Gunasekaran, 2005; Sharma, Munro, Dessev, Wiles, & Buwalda, 2016a; Sharma, Munro, Dessev, & Wiles, 2016b). These studies focussed mainly on the effect of processing or formulation on melt functionality.

Sharma et al. (2016a) studied the steady shear rheology of model Mozzarella cheeses manufactured in a twin screw Blentech cooker with shear work input as a major variable. Steady shear viscosity increased exponentially with shear work input indicating strong work thickening. Very high shear work inputs led to macroscopic structural breakdown of the cheese network with disappearance of the fibrous structure, loss of stretch, serum syneresis and decrease in melt functionality. These phenomena were attributed mainly to an increase in the strength of protein-protein interactions. Steady shear viscosity was negatively correlated with melt functionality. Sharma et al. (2016b) studied the oscillatory rheology of the same set of model Mozzarella cheeses. Frequency sweeps indicated that the cheese transformed from a viscoelastic liquid to a viscoelastic solid upon working at 70 ^{o}C. A critical stage indicating viscoelastic transition during processing was identified at a shear work input of 58.2 $kJ.kg^{-1}$ at 150 rpm. Mulvaney et al. (1997) also emphasised that the viscoelastic properties of Mozzarella cheese were influenced by the thermomechanical treatment given in a stretcher-cooker.

Stress relaxation and creep-recovery are common tests used for exploring transient viscoelastic behavior of many materials (Mezger, 2011). Both tests are used to study time dependent rheology in the linear viscoelastic region and both apply mechanical models e.g. Kelvin-Voigt for creep behavior. Many studies have been conducted on Mozzarella type cheeses and similar casein-based materials using creep-recovery and stress relaxation methods (Subramanian, Muthukumarappan, & Gunasekaran, 2003; Muliawan & Hatzikiriakos, 2007; Manski, van der Zalm, van der Goot & Boom, 2008; Olivares, Zorrilla, & Rubiolo, 2009; Bähler, Nägele, Weiss, & Hinrichs, 2015). Creep tests are more common for cheese rheology, as they are easier to perform, can describe material behavior more practically and are the best way of obtaining zero-shear viscosity. Creep-recovery tests can also be used to study the internal structure of Mozzarella cheese and physicochemical changes with temperature and during ripening (Olivares et al., 2009).

The current study focuses on microstructural changes in model Mozzarella cheeses with varying shear work input using confocal laser scanning microscopy, fat particle size analysis and creep-recovery behavior as tools. Nonfat cheese was included in the study to observe microstructural changes occurring in the absence of fat.

2. Materials and methods

2.1. Materials

Frozen blocks (-20 ^{o}C) of renneted and acidified protein gel manufactured from skim milk with typically 50 g. 100 g^{-1} moisture and 46 g. 100 g^{-1} protein were obtained from Fonterra Research and Development Centre (FRDC) pilot plant, Palmerston North, NZ. The blocks were thawed for 1 day at 11 ^{o}C and ground in a Rietz grinder (Rietz Manufacturing, Santa Rosa, CA, USA) with 6 mm grind size. Fresh cream was obtained from FRDC on each trial day. Cheese salt (Dominion Salt, Mount Maunganui, New Zealand) and tri-sodium citrate (TSC) (Jungbunzlauer, Basel, Switzerland) were also added.

2.2. Manufacture of model mozzarella cheeses

Protein gel, cream, water and salt were mixed, cooked and worked together at 70 ^{o}C in a counter rotating twin-screw cooker (Blentech, model CC-0045, Blentech Corporation, Rohnert Park, CA, USA) for the manufacture of model Mozzarella cheeses (Sharma, et al., 2016a). Three versions of model cheeses were prepared – full fat, nonfat and full fat with 0.5 g. 100 g^{-1} tri-sodium citrate (TSC) as a chelating agent. The target composition of full fat cheese was 23 g. 100 g^{-1} fat, 21 g. 100 g^{-1} protein, 53 g. 100 g^{-1} moisture and 1.4 g. 100 g^{-1} salt. Nonfat cheese had the same protein to salt and protein to moisture ratios as full fat cheese. Detailed manufacturing methods, sampling times, sample storage conditions and product compositions are given by Sharma et al. (2016a). Each experiment was repeated with at least one month between runs to ensure that the effect of shear work was independent of variations in raw material. Shear work input was estimated by numerical integration of power-time curves (Sharma et al., 2016a). Shear work inputs ranged from 2.8 to 185 kJ.kg^{-1}.

2.3. Fat particle size distribution

The fat particle size distribution of cheeses was obtained by disrupting the cheese matrix with chelating solution A (Walstra, 1965) and measuring size distributions using light scattering on the Mastersizer 2000 (Malvern Instruments, Malvern, UK). The experimental protocol suggested by Lee, Anema, and Klostermeyer (2004) was used with some modifications. A representative sample was collected from at least three different locations in the cheese. Approximately 0.5 g cheese was added to 50 ml solution A and mixed by gentle swirling action to minimize shear effects. Solution A contained 0.375 g. 100 g^{-1} EDTA and 0.125 mL. 100 mL^{-1} Tween 20 at pH 10. Cheese samples were held for 16 h after solution A addition. Particle size measurements were performed at room temperature (21^{o}C). Refractive indices were taken as 1.33 for the deionised water dispersant and 1.46 for milk fat. Particle size data were reported as average volume weighted diameter ($D_{4,3}$).

2.4. Confocal scanning laser microscopy (CSLM)

Confocal microscopy was used to determine the microstructure of cheese samples. Slabs of ~12 x 4 mm were cut from the cheese samples in the longitudinal fibre direction using a sharp razor blade and were then transferred to a stud holder with polyethylene glycol on the surface. Samples were frozen at -20 °C and sectioned into 50 µm slices on a cryo-microtome. Slices were immediately transferred to glass slides, stained with 0.4 g. 100 mL^{-1} Nile red and 0.2 g. 100 mL^{-1} fast green (made in citifluor to minimise photobleaching) and covered with a coverslip. The sectioned samples were stored at 4 °C for at least 48 h before imaging to ensure uniform dye uptake. Confocal images were taken using a Zeiss LSM 510 META confocal microscope (Carl Zeiss AG, Oberkochen, Germany) with excitation wavelengths of 488 nm and 633 nm. Images were taken 15 µm below the cheese surface.

2.5. Transient viscoelastic measurements (Creep)

The transient viscoelastic behavior of model Mozzarella cheese was studied by conducting creep and recovery tests at 20 °C or 70 °C. Creep tests were performed on an Anton Paar MCR 301 rheometer (Anton Paar, Graz, Austria) with a 20 mm diameter serrated plate geometry (PP20/P2) and a Peltier temperature hood (H-PTD 200). Disc-shaped cheese samples of 20 mm diameter and ~2 mm thickness were prepared and equilibrated to test temperature as previously described by Sharma, Dessev, Munro, Wiles, Gillies, Golding, …, Janssen (2015) except that a 1 N normal force was used to define the measurement gap and also to ensure good contact with the upper rotating plate. A 25 Pa shear stress was applied for 1001 s and then removed. The cheese was allowed to recover its strain for 3000 s. The resultant strain was measured as a function of time during the creep and recovery phases. The applied shear stress (25 Pa) was confirmed to be well within the linear viscoelastic limit using dynamic rheological tests.

2.5.1 Kelvin-Voigt model

Creep behavior can be represented by a series of mechanical spring and dashpot elements. Four and six element Kelvin-Voigt models (also known as Burgers models) were fitted to the experimental creep data. The six element model comprises a Maxwell element (spring and dashpot in series) in series with two Kelvin elements (spring and dashpot in parallel) (Fig. 1). The Maxwell element adds the instantaneous compliance (spring) and zero shear viscosity controlling permanent deformation (dashpot). The creep phase was analysed to determine fit parameters and both the creep and recovery phases were then predicted with these fit parameters. Data is presented in the form of shear creep compliance (J) as outlined in Steffe (1996):

During the creep phase

$$J = f(t) = \frac{\gamma(t)}{\tau_0} \quad (1)$$

$$\gamma(t) = \frac{\tau_0}{G_0} + \frac{\tau_0}{G_1}\left(1 - e^{-\frac{t}{\lambda_1}}\right) + \frac{\tau_0}{G_2}\left(1 - e^{-\frac{t}{\lambda_2}}\right) + \frac{\tau_0}{\eta_0} \cdot t \quad (2)$$

$$J(t) = J_0 + J_1\left(1 - e^{-\frac{t}{\lambda_1}}\right) + J_2\left(1 - e^{-\frac{t}{\lambda_2}}\right) + \frac{1}{\eta_0} \cdot t \quad (3)$$

During the recovery phase

$$\gamma(t) = \gamma_{max} - \frac{\tau_0}{G_0} - \frac{\tau_0}{G_1}\left(1 - e^{-\frac{t}{\lambda_1}}\right) - \frac{\tau_0}{G_2}\left(1 - e^{-\frac{t}{\lambda_2}}\right) \quad (4)$$

Where

$\gamma(t)$= Shear strain at time t

γ_{max}= Maximum strain attained during creep phase

τ_0= Applied shear stress, Pa

G_0= Instantaneous shear modulus, Pa

J_0= Instantaneous shear compliance, Pa^{-1}

G_1& G_2= Viscoelastic moduli of two retarded elements, Pa

J_1 & J_2= Retarded compliances, Pa^{-1}

η_0= Zero-shear or Newtonian viscosity, Pa.s

λ_1 & λ_2 = retardation times of two retarded elements = $\frac{\eta_1}{G_1}$ and $\frac{\eta_2}{G_2}$, s

η_1 & η_2= Shear viscosity in viscoelastic region, Pa.s

The parameters were obtained from the experimental curves in a stepwise fashion. G_o was first calculated from 45 data points in the 0 - 0.85 s time range. η_0 was then calculated from 33 data points in the 420 – 975 s range. The final 4 parameters in equation 2 were obtained using the successive residual method in Excel. An alternative calculation method used non-linear regression in SigmaPlot (version 11.0) to obtain 5 of the parameters in equation 2 after η_0 had been determined as above and subtracted. The '5-parameter exponential rise to maximum model' within the global curve fitting wizard was used. The alternative method gave similar values of the 5 parameters with goodness of fit $r^2 > 0.99$ (level of significance 5%) indicating that the 6 element model fitted the experimental data well. Relative recovery of strain at the end of the recovery step was also calculated (Patel, Dumlu, Vermeir, Lewille, Lesaffer, & Dewettinck, 2015).

$$\% \text{ Relative recovery, } \gamma_r = \frac{\gamma_{max} - \gamma_{end}}{\gamma_{max}} . 100 \quad (5)$$

where γ_{end} is the strain at the end of the recovery phase.

3. Results

3.1. Microstructure of sheared model Mozzarella cheeses

Confocal images of the model Mozzarella cheeses manufactured with varied shear work inputs are presented in Figs. 2, 3 & 4 for 50, 150 and 250 rpm screw speeds, respectively. Shear work induced microstructural changes at 50 rpm screw speed appear to be minor or subtle. However, major changes in both fat and protein phases were observed for 150 and 250 rpm screw speeds. In the initial stages of mixing (shear work typically < 5kJ.kg^{-1}) milk fat can be seen in relatively large pools in the protein network (Fig.2, 1.3 & 2.9 kJ.kg^{-1} and Fig. 4, 3.5 kJ.kg^{-1}). At a macroscopic level at such low shear work values the cheese was runny, often with some buttery liquid present indicating that the cream was not yet well mixed into the structure (Sharma et al., 2016a). Such large milk fat pools would lead to excessive fat leakage upon cheese melting. With further mixing (shear work 6-15 kJ.kg^{-1}), a more typical mozzarella structure was observed (Fig. 2, 5.9 & 12.0 kJ.kg^{-1} and Fig. 3, 8.8 kJ.kg^{-1}). No unmixed creamy liquid was observed at a macroscopic level. For all microstructures at shear work <40 kJ.kg^{-1} striated or anisotropic protein network structures were observed with fat dispersed in the protein mainly in the form of channels or elongated fat droplets. Hot water stretching and kneading action in the traditional manufacture of Mozzarella type cheeses also converts the casein mass into smooth, elongated and aligned microfibers in the direction of stretch with elongated fat channels between the fibers (McMahon et al., 1999; Oberg, McManus, & McMahon, 1993).

Cheeses with shear work in the range 50-60 kJ.kg^{-1} showed microstructures where elongated fat structures had virtually disappeared. The structures were isotropic and the fat globule size was now much smaller (Fig. 3, 58.2 kJ.kg^{-1} and Fig. 4, 53.9 kJ.kg^{-1}). At the highest shear work inputs microstructures showed a very fine dispersion of fat particles and an isotropic structure. Fine micro-cracks were also observed indicating a brittle material (Fig. 3, 73.7 kJ.kg^{-1} and Fig. 4, 166 kJ.kg^{-1}). These overworked cheeses no longer showed a fibrous macrostructure, were mechanically brittle and lacked stretch (Sharma et al., 2016a).

3.2. Fat particle size distributions

Fat particle size distributions for all samples were either bimodal or trimodal distributions (Fig. 5a). The largest volumetric frequency peak near 35 μm and a smaller peak near 0.5 μm occurred for all 6 samples. The dominance of particles around 35 μm agrees with the confocal images. For the three samples at the highest shear work inputs a third peak in the range 2 – 4 μm is observed. At lower shear work values (<30 kJ.kg^{-1}) the proportion of smaller particles was lower and the overall span of the distribution was larger. Cheese with the lowest shear work input (3.3 kJ.kg^{-1}) showed a wide distribution with some very large particles (500 μm) that disappeared with further shear work input. Further increases in shear work input resulted in an increase in the proportion of smaller fat particle sizes and a narrowing in the width of the biggest peak (~35 μm). El-Bakry, Duggan, O'Riordan, and O'Sullivan (2011) also reported narrowing of the fat globule size distribution upon mixing of imitation cheese in a twin screw cheese cooker. The presence of large particles (500 μm) and tiny particles (< 1 μm) was not evident on the confocal images indicating the practical limits of confocal imaging - limited sample selection and particle resolution > 1 μm.

Mean fat particle size ($d_{4,3}$) decreased with shear work input (Fig. 5b). The mean fat particle size decreased from 45 μm to 20 μm as shear work input increased from 3.3 to 74 $kJ.kg^{-1}$.

3.3. Transient viscoelastic properties

Creep and recovery was used to study the transient viscoelastic nature of the model cheeses. Three distinct regions are visible in the creep phase of all the cheeses (Fig.6). These regions are instantaneous elastic deformation, viscoelastic or delayed elastic deformation and pure viscous creep. The strain during the first two regions (elastic and viscoelastic) is expected to be fully recovered whereas the strain from the last region (viscous flow) will result in permanent deformation. The relative contribution of the regions changed as shear work input increased. For all cheeses, a significant contribution of viscous flow to overall creep is observed as there was always residual permanent deformation even 3000 s after shear stress was removed.

Table 1 shows maximum shear strain (γ_{max}), relative recovery of shear strain and fitted creep parameters using a 6-element Burger's model. γ_{max} decreased with shear work input. For shear work < 30 $kJ.kg^{-1}$, γ_{max} was in the range of 0.0076-0.01. At the highest shear work input γ_{max} was 0.0051. Lower levels of γ_{max} indicate hardening of the material. γ_{max} was higher for nonfat cheese (0.011) and higher again for full fat cheese with TSC added (0.016). This indicates that nonfat cheese and TSC full fat cheese were softer than their full fat counterpart.

The extent of shear strain recovery should indicate the relative proportion of elastic components (instantaneous strain and delayed elasticity) in the cheeses. A high proportion of viscous creep will give a low relative recovery of shear strain. For shear work inputs in the range 3-58 kJ.kg^{-1}, strain recovery was in the range of 57-65% (Fig. 6a and Table 1). However, for the excessively worked sample (74 kJ.kg^{-1}) the recovery was much higher (85%). This indicates a significant decrease in the viscous flow component for excessively worked full fat cheese. This is expected given its much higher steady shear viscosity (Sharma et al, 2016a). At similar shear work inputs (3-9 kJ.kg^{-1}), nonfat cheese exhibited a higher shear strain recovery than full fat cheese (Table 1). Fat at 20 ^{o}C is known to undergo plastic deformation contributing to permanent deformation. Nonfat cheese is therefore more elastic. Cheese with TSC added showed the lowest strain recovery of any of the cheeses. Chelation of salts such as calcium by TSC gives this cheese a lower steady shear viscosity (Sharma et al, 2016a) so there is a higher viscous creep.

From the six elements of the Burger's model three represent elastic behavior, i.e. time-independent instantaneous compliance (J_0) and time dependent retarded compliances (J_1 and J_2). J_0 represents the Hookean spring element which is related to the undisturbed cheese structure consisting of a protein network and partially solidified fat (Olivares et al., 2009; Subramanian et al, 2003). The protein network in cheese is regarded as the major contributing factor to the elastic behavior. Higher values of J_0 indicate less rigidity meaning that the protein network is relatively free to rearrange between crosslinks (Olivares et al., 2009) and the material shows higher deformations. J_0 for the full fat model cheeses (2.67-4.18 x10^{-5} Pa^{-1}) showed no definite trend with increase in shear work input (Table 1). J_0 for nonfat cheese was higher than that for full fat cheese indicating less rigidity.

J_1 and J_2 are the major components of the viscoelastic behavior of model Mozzarella cheese (Subramanian et al., 2003). J_2 indicates the size of the fast viscoelastic deformations whereas J_1 indicates the size of the slower viscoelastic deformations. J_2 does not vary systematically with shear work. The decrease in J_1 with increasing shear work input indicates an increase of rigidity (Table 1). Values of both J_1 and J_2 were higher for nonfat cheese and cheese with TSC added than for full fat cheese suggesting a higher viscoelastic component to the response and a lower rigidity.

Retardation time (λ) is another important parameter in viscoelastic behavior. It quantifies the delayed response to applied stress and can be linked to delayed elasticity (Mezger, 2011). λ_2 was in the range 3.3-5.1s and λ_1 in the range 129-193 s for all three types of model cheeses. No trends were evident for either λ_1 or λ_2 as a function of either shear work input or model cheese type. However, it was evident that J_1 decreased and η_1 increased with shear work input suggesting an increase in both elastic and viscous behavior. Retardation time is inversely related to network elasticity. Therefore, more elastic material should have smaller retardation times, while softer materials tend to have longer retardation times. Maybe the changes in J_1 and η_1 are such that no significant changes in retardation time occur.

η_0 measured by the creep method corresponds to the zero shear viscosity as the shear rates in this region are very low (10^{-6} s^{-1}). η_0 increased exponentially with shear work input. Steady shear viscosity at higher shear rates also increased exponentially with shear work input (Sharma et al., 2016a). The exponential increase in viscosity during mixing and working of model Mozzarella cheese is linked with the increased strength of the protein matrix either because of more protein-protein bonds or an increase in their strength.

The 6-element Burger's model with parameters calculated from the creep phase data fits experimental data in the creep phase very well (Fig. 7). These parameters also fit experimental data for the first 500 s of the recovery phase, but do not fit adequately in the later stages. The experimental data indicates a higher recovery of applied strain than the model predicts. Fitting a 6 element model to the data for just the recovery phase also gives good curve fits but with much longer time constants than those in Table 1, e.g. 50 s and 990 s for full fat cheese with 4.3 $kJ.kg^{-1}$ shear work input.

At 70 ^{o}C the creep curve (Fig. 8) for full fat cheese indicated that overall deformation was dominated by pure viscous flow causing a high amount of permanent deformation with only 48% strain recovery. A 4-element Burger's model was found to fit the experimental data well. The following creep function was obtained at 70 ^{o}C after applying 0.05 Pa shear stress.

$$J(t) = 1.25 \times 10^{-4} + 3.71 \times 10^{-2} \left(1 - e^{-\frac{t}{10.46}}\right) + \frac{1}{491} \cdot t \qquad (6)$$

Compared to data for the same sample at 20 ^{o}C J_0 is 3 times higher and J_1 is 366 times higher indicating a much less rigid structure. η_1 is 0.00018 times and η_0 is 0.000088 times that at 20 ^{o}C. At 70 ^{o}C both fat and protein phases are molten and therefore contribute significantly to viscous flow but the viscosity is much lower. Only one retardation time of 10.46 s is needed to represent the behavior at 70 ^{o}C.

4. Discussion

For any model cheese or imitation cheese where the fat and protein are added as separate phases mixing is a crucial part of structure development at both the macroscopic and microscopic levels. Because of the very high viscosity of the molten cheese and the low Reynolds number (Re < 0.1) the mixing will be laminar rather than turbulent. In laminar mixing of two phases of roughly similar volume the essential mechanism of structure development is layering, stretching and folding which leads to striated structures (Szalai, Alvarez, & Muzzio, 2004) such as those in Fig. 2 and also at low shear work in Figs. 3 & 4. This striation mechanism combined with the fiber forming properties of renneted casein leads to the formation of a typical Mozzarella structure with the right characteristics to have good pizza functionality. In our experiments the layering, stretching and folding is generated by the mixing action of the twin augers in the Blentech cooker.

The presence of pockets that combine fat and serum in traditional Mozzarella type cheeses is well reported (Paulson, McMahon, & Oberg, 1998; McMahon et al., 1999; Mizuno & Lucey, 2005; McMahon, Paulson, & Oberg, 2005). The laminar mixing action of the augers creates similar, desirable striated protein structures with optimum sized fat-serum channels to give good melt functionality (Sharma et al., 2016a). These striated structures are the basis for the mechanical and structural anisotropy observed in fat-protein networks (Cervantes, Lund, & Olson, 1983; Ak and Gunasekaran, 1997; Manski et al., 2008; Bast et al., 2015; Sharma et al., 2015).

Further mixing (shear work input >58 kJ.kg^{-1}) resulted in striation break up, a more uniform distribution of fat within the protein network, the disappearance of anisotropic fiber structures (Figs 3 & 4), much finer fat particles (Fig. 5) and poor melt (Sharma et al., 2016a). El-Bakry et al. (2011) also reported the disappearance of the microscopic fibrous character of imitation cheese with processing time and noted a honeycomb structure with prolonged working. Excessive working (>74 kJ.kg^{-1}) eventually led to the breakdown of the protein matrix showing an aggregated macroscopic structure accompanied by loss of serum fluid (Sharma et al., 2016a). Confocal images indicated a brittle material with microcracks present (Figs. 3 & 4). Excessive protein-protein interactions mediated by calcium ions can be related to the formation of these aggregated structures and the expulsion of serum (McMahon et al., 1999; Sharma et al., 2016b).

The very large fat particles (500 μm) observed at low shear work input disappeared at higher shear work values (Fig. 5a). This rapid reduction of fat particle size suggests effective dispersive mixing in the initial working phases. Excessive working led to the occurrence of many more submicron fat particles (Fig. 5a). The fat particle size distribution after working molten cheese in twin screw cookers is expected to result from a dynamic equilibrium between particle break up by shear and particle growth by coalescence. The results indicate that particle break up by shear is dominant as $d_{4,3}$ continuously decreased with increasing shear work input (Fig. 5b). Coalesence may be increasing at high shear work levels as the curve flattens (Fig. 5b).

The changes in creep and recovery behavior at 20 ^{o}C of full fat model cheese with increasing shear work input broadly agree with the changes reported in steady shear viscosity (Sharma et al., 2016a) and oscillatory rheology (Sharma et al., 2016b). Steady shear viscosity increased exponentially with shear work input (Sharma et al., 2016a) and η_0 also increased exponentially with shear work input (Table 1). Frequency sweeps indicated a more elastic, solid-like structure with increasing shear work input (Sharma et al., 2016b) and decreasing J_1 and increasing η_1 with increasing shear work input (Table 1) also indicate more elastic, solid-like behavior. The comparison between full fat cheese, nonfat cheese and TSC added cheese from the creep and recovery behavior also agrees with previous work. At a similar shear work level full fat cheese is harder (lower γ_{max}, Table 1) and more rigid (lower J_0, Table 1) than the other two cheeses and had lower frequency dependence indicating a harder, more solid-like structure (Sharma et al., 2016b). η_0 was lowest for TSC added cheese whereas full fat and nonfat cheeses had similar η_0. Full fat cheese and nonfat cheeses had similar steady shear viscosities but that for TSC added cheese was lower (Sharma et al., 2016a).

The retardation times (λ_1 & λ_2) are time constants for the viscoelastic changes in the Kelvin elements in the model (Fig. 1). Retardation times are useful in the design of cheese forming devices such as block formers or extrusion processes. A useful rule of thumb is that the timescale of deformation must be longer than the retardation time if changes in shape are to be permanent. When processing at 70 °C holding of a new shape for at least 11 s is therefore necessary for a permanent shape change. At 20 °C two retardation times were needed to model the behavior (Table 1). For all cheeses J_1 was 2 to 3 times J_2 so the longer retardation time λ_1 is more important to permanent shape change than λ_2. A holding time of 150 – 200 s is therefore needed for a permanent shape change at 20 °C .

The retardation times reported here are the same order of magnitude as those reported for a cheese like material, shear structured and transglutaminase cross-linked 30 % calcium caseinate in the presence of palm fat, at 20 °C (Manski et al., 2008). Their 6-element Burgers model gave retardation times of 8-11 s and 200-260 s compared to our values of 3-5 s and 130-193 s.

Sharma et al. (2016b) proposed a schematic model to describe structural changes in model Mozzarella cheeses as they were progressively sheared. The model showed the fat phase changing from large, elongated particles at low shear work input (< 30 kJ.kg^{-1}), to smaller elongated fat particles at 58 kJ.kg^{-1}, to small, spherical fat particles at > 70 kJ.kg^{-1}. The changes in fat particle size distribution and fat microstructure reported here add further experimental support for the model.

5. Conclusions

Mozzarella cheese is a pasta-filata variety of cheese that undergoes through kneading and stretching action during working giving rise to typical fibrous appearance. The energy imparted to cheese during working in the form of shear work shall govern its structure, rheology and functionality. Our work demonstrated that shear work input has huge impact on the fat particle size, structure and rheology of a model Mozzarella cheese. It also elucidates importance of the stretching-folding action in Blentech (twin screw cooker) for the formation of striated anisotropic structure. Furthermore, prolonged shearing of cheese samples causes significant changes in the microstructure from an anisotropic structure with aligned fat-serum channels to an isotropic, more elastic structure with presence of small fat globules and some micro-cracks. This study hypothesizes that shear wok induced changes are led by changes in protein phase; however, future systematic studies are required on quantification of structural changes in protein phase.

Acknowledgements

The authors thank Fonterra Co-operative Group and the Ministry for Primary Industries, NZ for funding this project under the Dairy Primary Growth Partnership programme in Food Structure Design. Authors thank Robbie Buwalda, Bhavin Parmar, Ben Somerton, Grant Bleakin, Dave Griffin and Ken Anderson for their help with the Blentech trials at FRDC. Authors also thank Elizabeth Nickless, FRDC for helping with confocal laser scanning microscopy analysis of cheese samples. Statistical help received from Maria Ferrua, Riddet Institute, for helpful discussions on the best methods for fitting models to experimental data is duly acknowledged.

References

Ak, M.M., & Gunasekaran, S. (1997). Anisotropy in tensile properties of mozzarella cheese. *Journal of Food Science, 62,* 1031-1033.

Bähler, B., Nägele, M., Weiss, J., & Hinrichs, J. (2016). Temperature and time-dependent relaxation of compressed cheese curd cubes: effect on structuring of pasta-filata cheese. *Journal of Texture Studies*, *47*, 58-67.

Bast, R., Sharma, P., Easton, H.K.B., Dessev, T.T., Lad, M., & Munro, P.A. (2015). Tensile testing to quantitate the anisotropy and strain hardening of Mozzarella cheese. *International Dairy Journal, 44,* 6-14.

Cervantes, M.A., Lund, D.B., & Olson, N.F. (1983). Effects of salt concentration and freezing on Mozzarella cheese texture. *Journal of Dairy Science, 66,* 204-213.

El-Bakry, M., Duggan, E., O'Riordan, E. D., & O'Sullivan, M. (2010a). Effects of emulsifying salts reduction on imitation cheese manufacture and functional properties. *Journal of Food Engineering, 100*, 596-603.

El-Bakry, M., Duggan, E., O'Riordan, E. D., & O'Sullivan, M. (2010b). Small scale imitation cheese manufacture using a Farinograph. *LWT-Food Science and Technology, 43,* 1079-1087.

El-Bakry, M., Duggan, E., O'Riordan, E. D., & O'Sullivan, M. (2011). Casein hydration and fat emulsification during manufacture of imitation cheese, and effects of emulsifying salts reduction. *Journal of Food Engineering, 103,* 179-187.

Glenn, T. A., Daubert, C. R., Farkas, B. E., & Stefanski, L. A. (2003). A statistical analysis of creaming variables impacting process cheese melt quality. *Journal of Food Quality, 26,* 299-321.

Kapoor, R., Lehtola, P., & Metzger, L. E. (2004). Comparison of pilot-scale and rapid visco analyzer process cheese manufacture. *Journal of Dairy Science*, *87*, 2813-2821.

Lee, S. K., Anema, S., & Klostermeyer, H. (2004). The influence of moisture content on the rheological properties of processed cheese spreads. *International Journal of Food Science and Technology*, 39, 763–771.

Manski, J.M., van der Zalm, E.E.J., van der Goot, A.J., & Boom, R.M. (2008). Influence of process parameters on formation of fibrous materials from dense calcium caseinate dispersions and fat. *Food Hydrocolloids, 22,* 587-600.

McMahon, D. J., Fife, R. L., & Oberg, C. J. (1999). Water partitioning in Mozzarella cheese and its relationship to cheese meltability. *Journal of Dairy Science*, *82*, 1361–1369.

McMahon, D. J., Paulson, B., & Oberg, C. J. (2005). Influence of calcium, pH, and moisture on protein matrix structure and functionality in direct-acidified nonfat Mozzarella cheese. *Journal of Dairy Science*, *88*, 3754-3763.

Mezger, T.G. (2011). *The Rheology Handbook: for Users of Rotational and Oscillatory Rheometers*. (3rd ed.). Hannover, Germany: Vincentz Network GmbH & Co.

Mizuno, R., & Lucey, J. A. (2005). Effects of emulsifying salts on the turbidity and calcium-phosphate-protein interactions in casein micelles. *Journal of Dairy Science, 88,* 3070–3078.

Muliawan, E.B., & Hatzikiriakos, S.G. (2007). Rheology of Mozzarella Cheese. *International Dairy Journal*, *17*, 1063-1072.

Mulvaney, S., Rong, S., Barbano, D. M., & Yun, J. J. (1997). Systems analysis of the plasticization and extrusion processing of Mozzarella cheese. *Journal of Dairy Science*, *80,* 3030-3039.

Noronha, N., O'Riordan, E. D., & O'Sullivan, M. (2008). Influence of processing parameters on the texture and microstructure of imitation cheese. *European Food Research and Technology, 226*, 385-393.

Oberg, C. J., McManus, W. R., & McMahon, D. J. (1993). Microstructure of Mozzarella cheese during manufacture. *Food Structure, 12*, 251-258.

Olivares, M.L., Zorrilla, S.E. & Rubiolo, A.C. (2009). Rheological properties of mozzarella cheese determined by creep/recovery tests: effect of sampling direction, test temperature and ripening time. *Journal of Texture Studies, 40,* 300-318.

Patel, A. R., Dumlu, P., Vermeir, L., Lewille, B., Lesaffer, A., & Dewettinck, K. (2015). Rheological characterization of gel-in-oil-in-gel type structured emulsions. *Food Hydrocolloids*, 46, 84-92.

Paulson, B. M., McMahon, D. J., & Oberg, C. J. (1998). Influence of sodium chloride on appearance, functionality, and protein arrangements in nonfat Mozzarella cheese. *Journal of Dairy Science, 81,* 2053–2064.

Sharma, P., Dessev, T.T., Munro, P.A., Wiles, P.G., Gillies, G., Golding, M., James, B. & Janssen, P. (2015). Measurement techniques for steady shear viscosity of Mozzarella-type cheeses at high shear rates and high temperature. *International Dairy Journal*, 47, 102-108.

Sharma, P., Munro, P.A., Dessev, T.T., Wiles, P.G., & Buwalda, R.J. (2016a). Effect of shear work input on steady shear rheology and melt functionality of model Mozzarella cheeses. *Food Hydrocolloids*, 54, 266-277.

Sharma, P., Munro, P.A., Dessev, T.T. & Wiles, P.G. (2016b). Shear work induced changes in the viscoelastic properties of model Mozzarella cheese. *International Dairy Journal*, 56, 108-118.

Steffe, J. F. (1996). *Rheological methods in food process engineering* (2nd ed.). East Lansing, MI, USA: Freeman Press.

Subramanian, R., Muthukumarappan, K., & Gunasekaran, S. (2003). Effect of methocel as a water binder on the linear viscoelastic properties of mozzarella cheese during early stages of maturation. *Journal of Texture Studies, 34*, 361-380.

Szalai, E.S., Alvarez, M.M., & Muzzio, F.J. (2004). Laminar mixing: a dynamical systems approach. In E.L. Paul, V.A. Atiemo-Obeng, & S.M. Kresta (Eds.), *Handbook of industrial mixing: Science and practice* (pp. 89-143). Hoboken, NJ: Wiley.

Walstra, P. (1965). Light scattering by milk fat globules. *Netherlands Milk and Dairy Journal*, 19, 93–109.

Yu, C., & Gunasekaran, S. (2005). A systems analysis of pasta filata process during Mozzarella cheese making. *Journal of Food Engineering*, *69*, 399-408.

Table

Table 1. Fitted creep parameters obtained for model Mozzarella cheeses using a 6-element Burgers model*.

Cheese Type	Shear work (kJ.kg^{-1})	Maximum shear creep (γ_{max})	Relative recovery of shear strain (%)	J_0 (10^{-5} Pa^{-1})	J_1 (10^{-5} Pa^{-1})	η_1 (10^6 Pa.s)	λ_1 (s)	J_2 (10^{-5} Pa^{-1})	η_2 (10^5 Pa.s)	λ_2 (s)	η_0 (10^6 Pa.s)
Full fat	3.3	0.0097	56.9	3.29	9.91	1.32	129.71	2.47	1.01	3.32	4.49
	4.3	0.0079	59.9	2.67	8.88	2.17	191.17	2.93	1.39	4.11	5.95
	8.8	0.0089	64.9	4.18	10.1	1.57	158.89	4.25	0.93	4.00	5.57
	26.3	0.0076	64.7	3.09	8.45	1.81	153.08	4.16	1.21	5.05	5.98
	58.2	0.0066	60.1	3.14	7.73	2.11	160.27	4.31	1.17	5.01	7.99
	73.7	0.0051	84.9	2.96	5.64	2.74	153.66	2.95	1.36	3.95	12.10
Nonfat	6.8	0.0113	70.3	5.32	12.0	1.61	193.03	6.46	0.69	4.52	4.74
TSC added full fat	4.4	0.0157	54.8	4.72	16.8	1.00	170.31	4.82	0.72	3.75	2.79

* 25 Pa of shear stress was applied at 20 °C for 1001 s. The recovery phase was 3000 s. The parameters are defined in section 2.5.1.

Data represents the average of two measurements on the same sample.

Figure

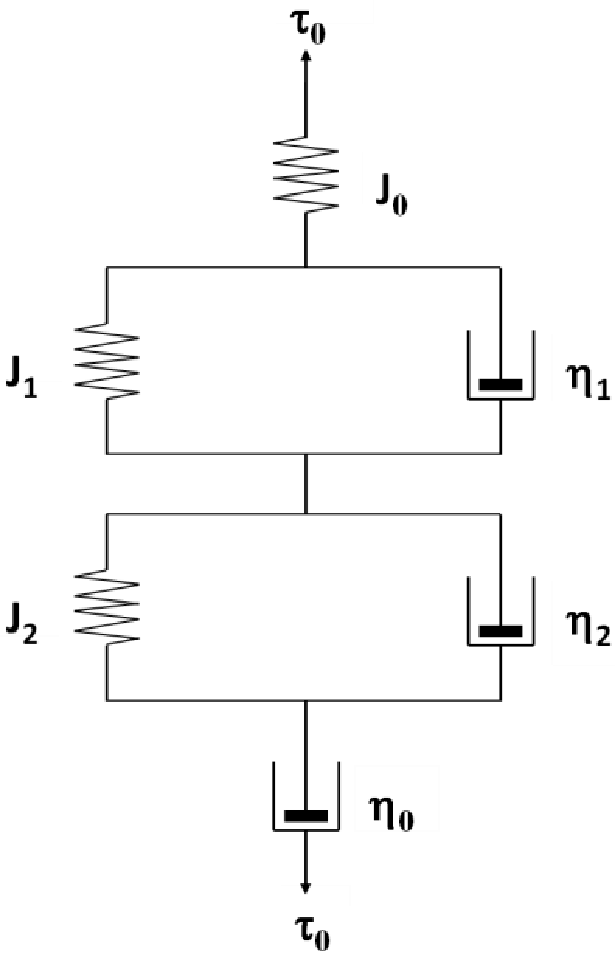

Fig. 1. Six-element linear viscoelastic mechanical model used for describing creep and recovery behaviour of model Mozzarella cheeses. The model parameters are defined in section 2.5.1

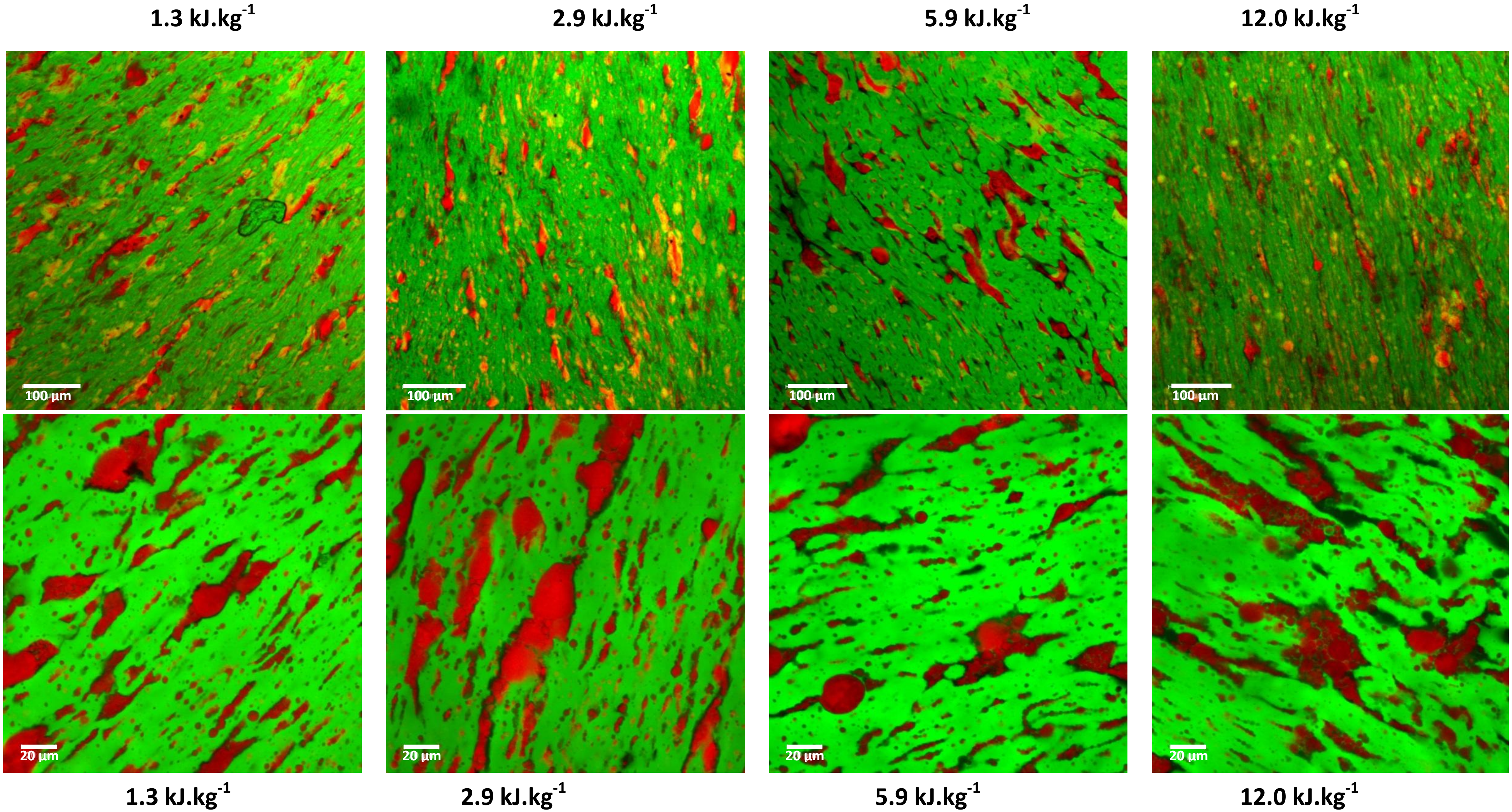

Fig. 2. Confocal laser scanning microscopic images of model Mozzarella cheeses subjected to different amounts of shear work. Shear work inputs are noted on the micrographs. Model Mozzarella cheeses were manufactured in the Blentech cooker at 50 rpm screw speed (Day 2) and 70°C. Red – fat, green – protein, black - air or water.

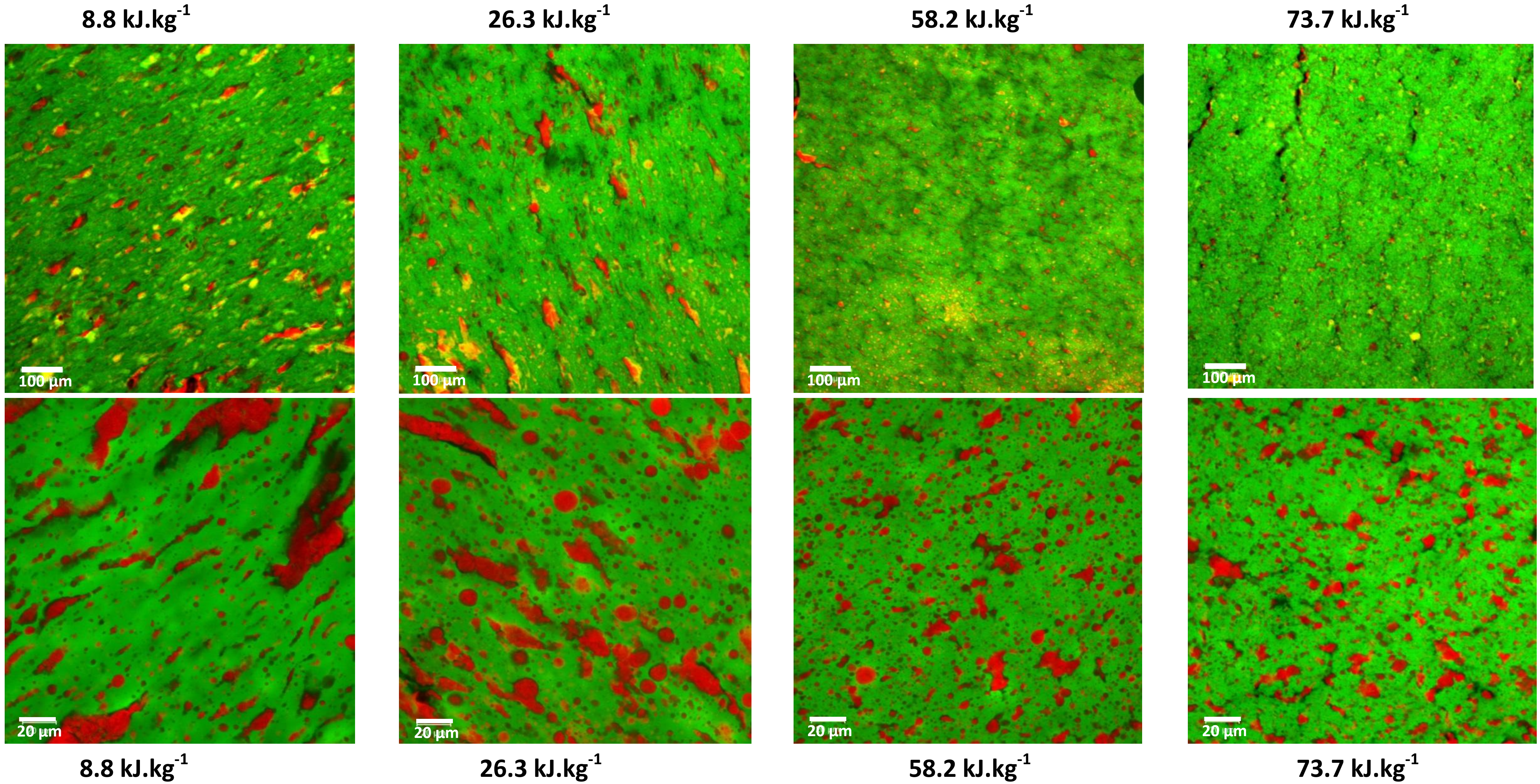

Fig. 3. Confocal laser scanning microscopic images of model Mozzarella cheeses subjected to different amounts of shear work. Shear work inputs are noted on the micrographs. Model Mozzarella cheeses were manufactured in the Blentech cooker at 150 rpm screw speed (Day 1) and 70^{o}C. Red – fat, green – protein, black - air or water.

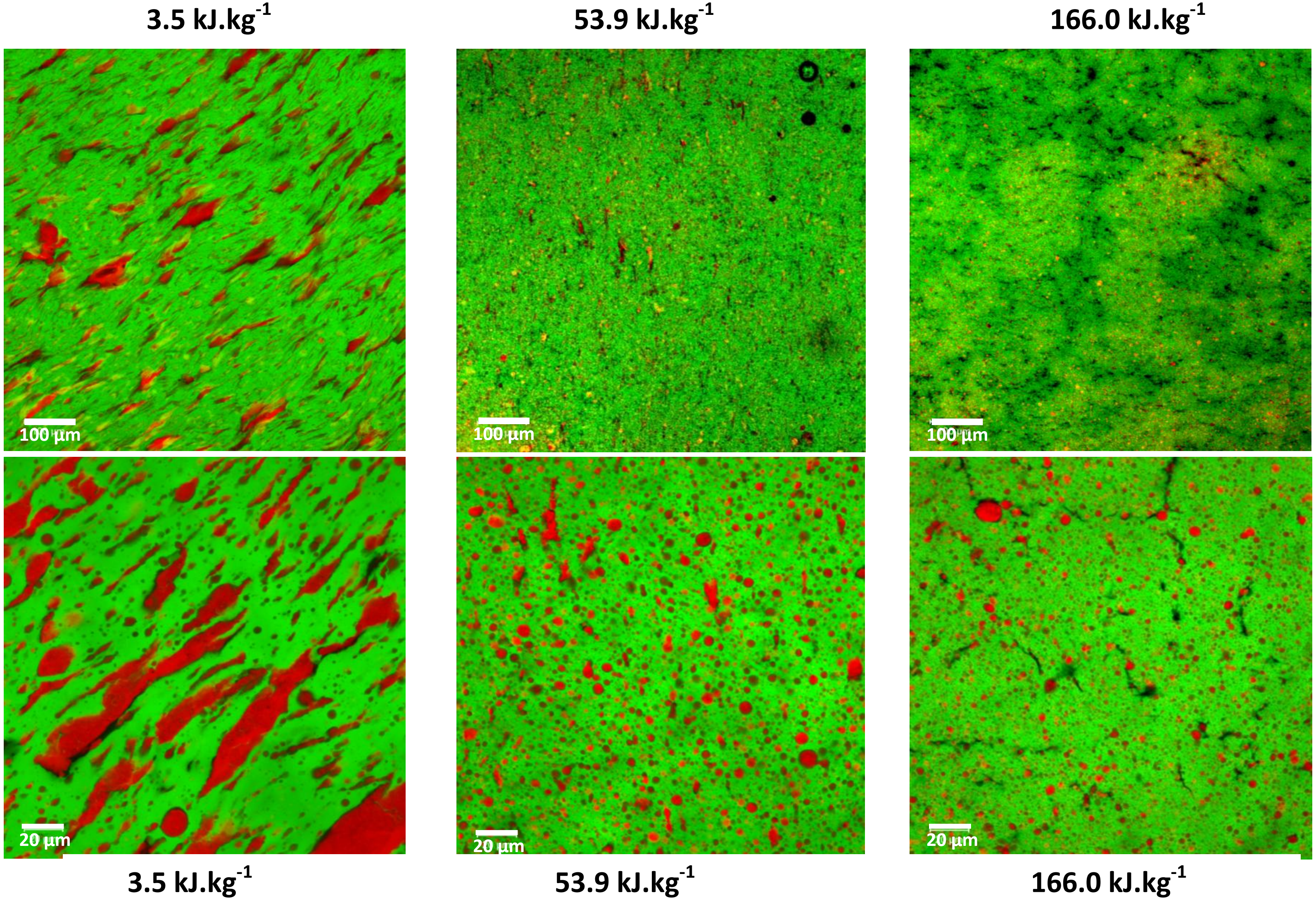

Fig. 4. Confocal laser scanning microscopic images of model Mozzarella cheeses subjected to different amounts of shear work. Shear work inputs are noted on the micrographs. Model Mozzarella cheeses were manufactured in the Blentech cooker at 250 rpm screw speed (Day 1) and 70°C. Red – fat, green – protein, black - air or water.

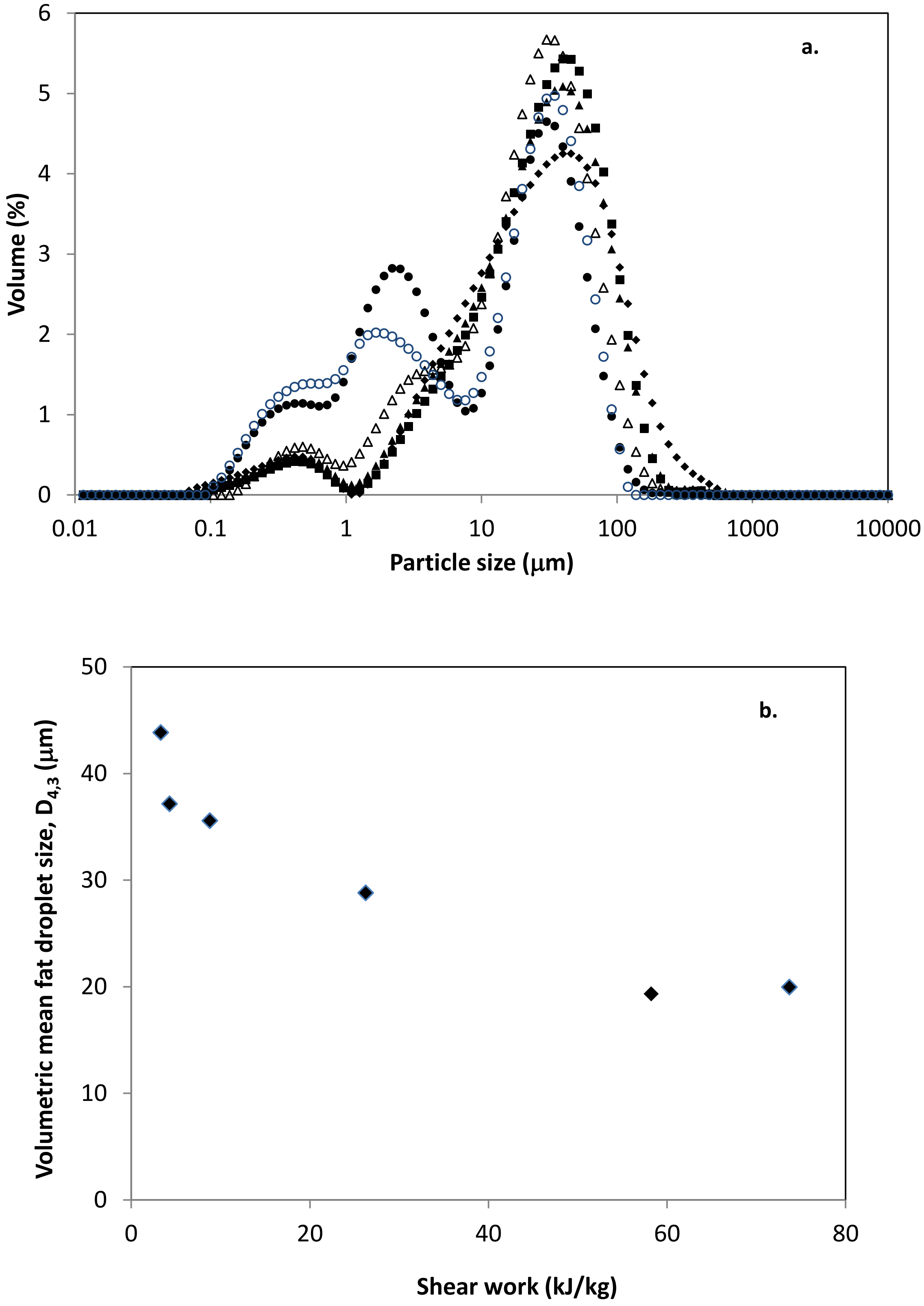

Fig.5. Effect of shear work on fat particle size of model Mozzarella cheese. a. Fat particle size distributions of model cheeses having varied shear work input, 3.3 kJ.kg^{-1} (♦), 4.3 kJ.kg^{-1} (■), 8.8 kJ.kg^{-1} (▲), 26.3 kJ.kg^{-1} (Δ), 58.2 kJ.kg^{-1} (•), 73.7 kJ.kg^{-1} (o); b. Volumetric mean fat particle size (♦) versus shear work input. Model Mozzarella cheeses were manufactured in the Blentech cooker at 150 rpm screw speed (Day 1) and 70^{o}C. Data represents the average of two measurements on the same sample.

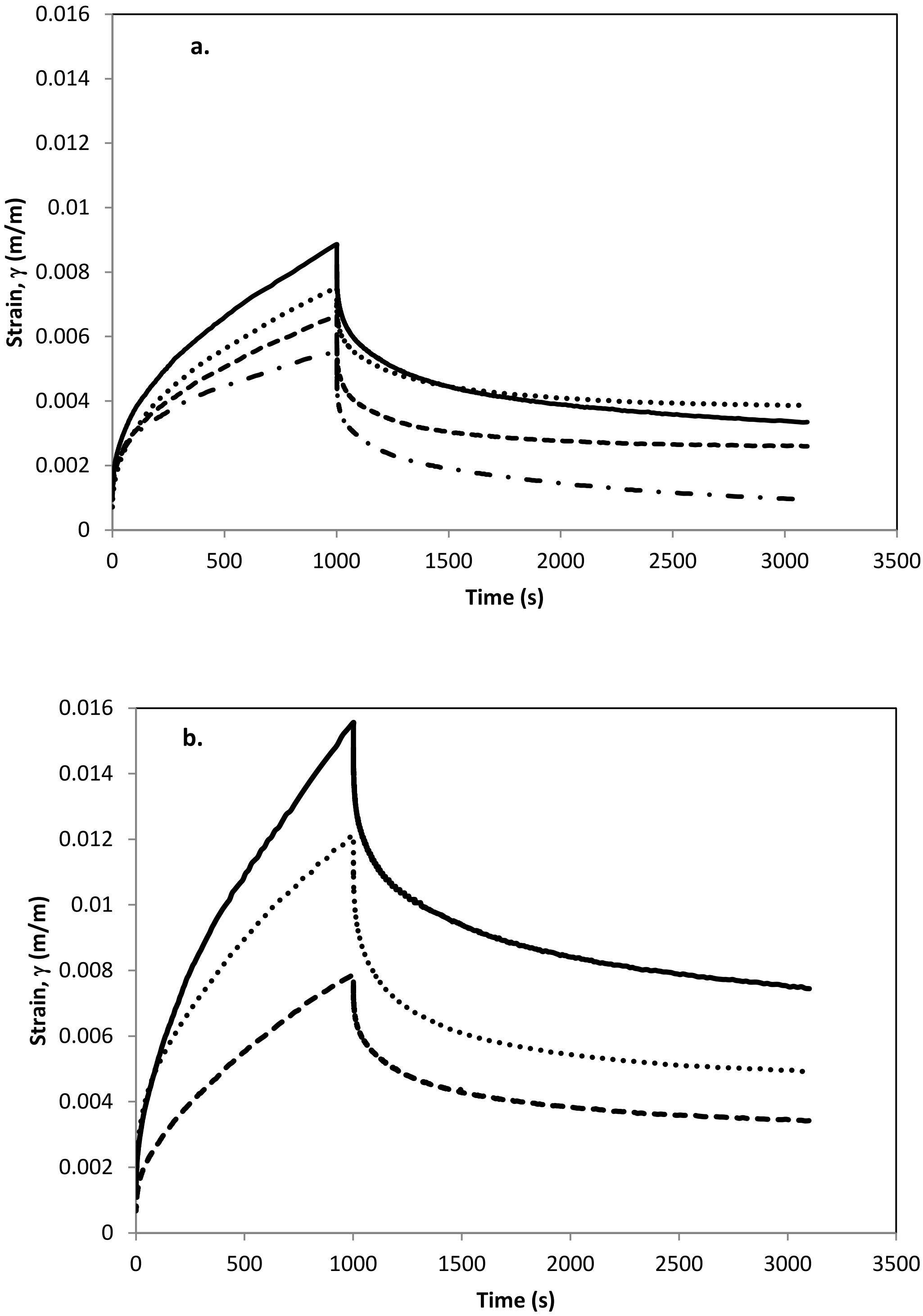

Fig. 6. Creep and creep recovery curves of model Mozzarella cheeses at 20°C. Applied shear stress was 25 Pa (within the linear viscoelastic limit). a. Full fat cheeses having different shear work input, 8.8 kJ.kg^{-1} (—), 26.3 kJ.kg^{-1} (●●●), 58.2 kJ.kg^{-1}(– – –), 73.7 kJ.kg^{-1} (— ● —); b. Full fat cheese- 4.3 kJ/kg^{-1} (— — —), TSC added cheese- 4.4 kJ.kg^{-1} (—) and nonfat cheese- 6.8 kJ.kg^{-1} (●●●) with similar shear work input. Model Mozzarella cheeses were manufactured in the Blentech cooker at 150 rpm screw speed and 70°C.

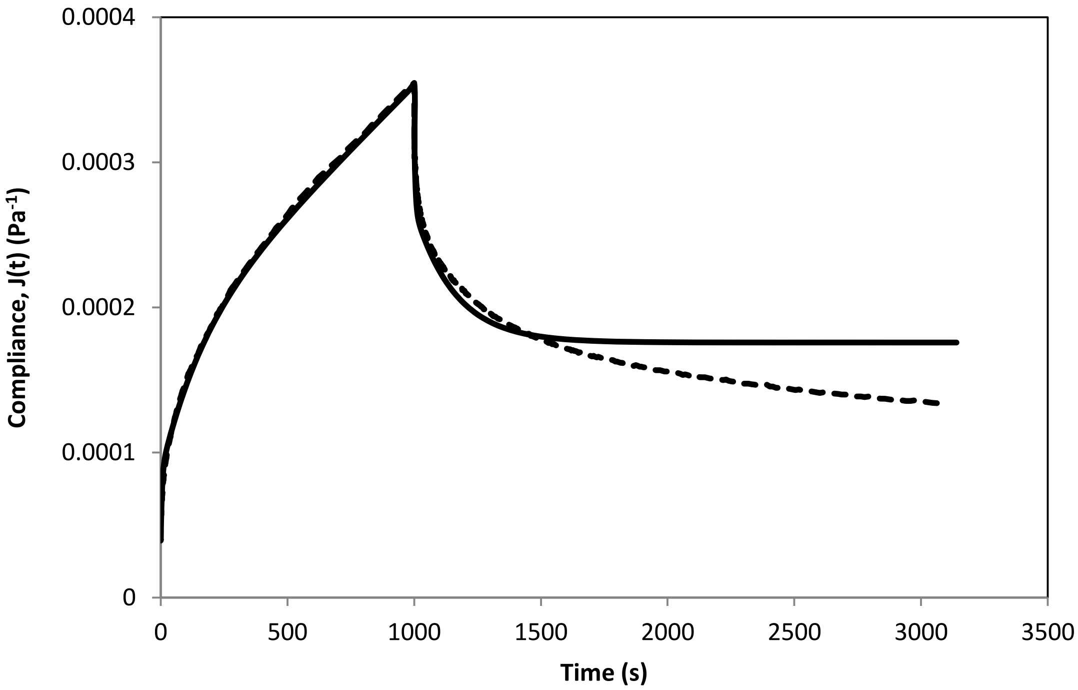

Fig. 7. Creep and recovery compliance data (Dashed line) and fitted curve (solid line) of model Mozzarella cheese at 20°C. Applied shear stress was 25 Pa (within the linear viscoelastic limit). The fitted curve was obtained from predicted values of compliance using a 6-element Burger's model with parameters calculated for the creep phase only. The model cheese had 8.8 kJ.kg^{-1} of shear work input and was manufactured in the Blentech cooker at 150 rpm screw speed and 70°C.

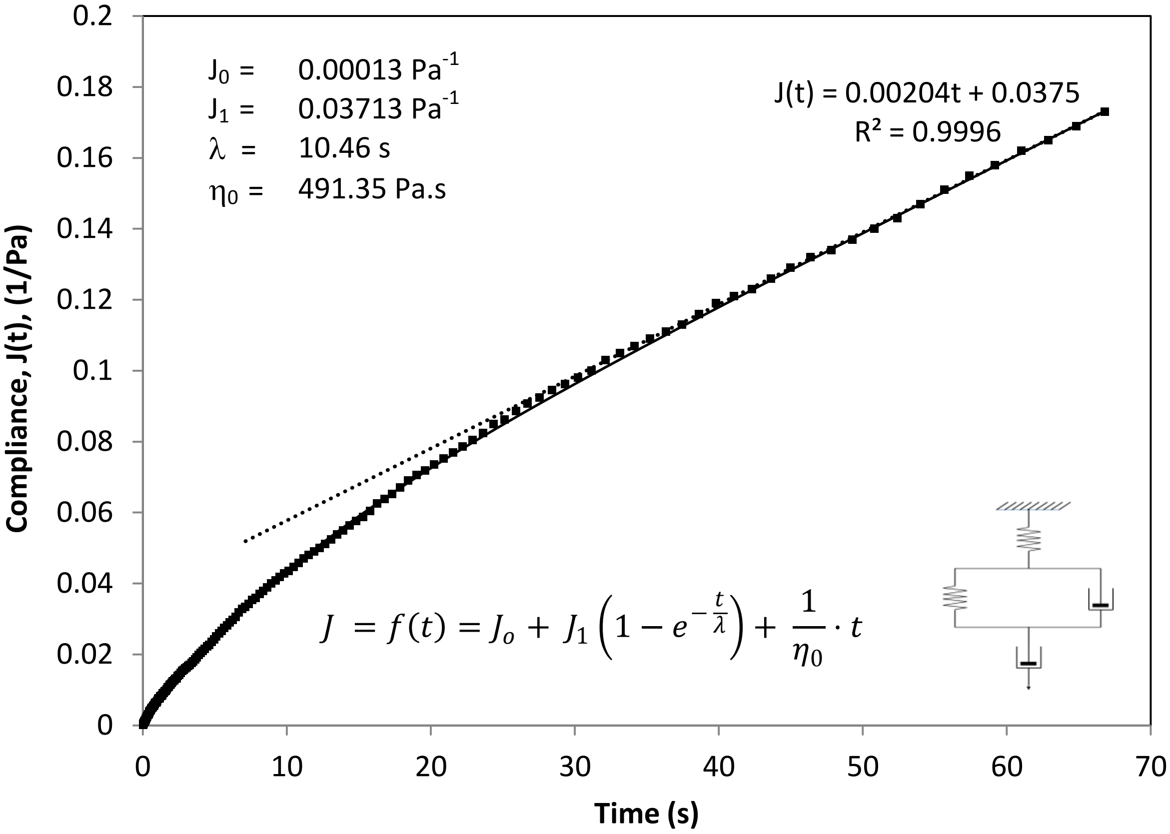

Fig. 8. Creep compliance data (■) and fitted curve (continuous line) of model Mozzarella cheese at 70°C. Applied shear stress was 0.05 Pa. (within the linear viscoelastic limit). The fitted curve used a 4-element Burger's model. Zero shear viscosity (η_0) was calculated from the linear regression line (dotted) in the later part of creep. The model cheese had 8.8 $kJ.kg^{-1}$ of shear work input and was manufactured in the Blentech cooker at 150 rpm screw speed and 70°C.